Microchimica Acta (2019) 186: 667
https://doi.org/10.1007/s00604-019-3755-4

REVIEW ARTICLE

Gold and silver nanoparticles in resonance Rayleigh scattering techniques for chemical sensing and biosensing: a review

Riham El-Kurdi[1] · Digambara Patra[1]

Received: 18 April 2019 / Accepted: 10 August 2019 / Published online: 4 September 2019

Abstract
This review (with 116 refs.) summarizes the state of the art in resonance Rayleigh scattering (RRS)-based analytical methods. Following an introduction into the fundamentals of RRS and on the preparation of metal nanoparticles, a first large section covers RRS detection methods based on the use of gold nanoparticles, with subsections on proteins (albumin, bovine serum albumin and ovalbumin, glycoproteins, folate receptors, iron binding-proteins, G-proteins-coupled receptors, transmembrane proteins, epidermal growth factor receptors), on pesticides, saccharides, vitamins, heavy metal ions (such as mercury, silver, chromium), and on cationic dyes. This is followed by a section on RRS methods based on the use of silver nanoparticles, with subsections on the detection of nucleic acids and insecticides. Several Tables are presented where an RRS method is compared to the performance of other methods. A concluding section summarizes the current status, addresses current challenges, and gives an outlook on potential future trends.

Keywords Nanomaterials · RRS · Nanoprobes · Determination · Spectroscopy · Bioanalysis · Heavy metals · Synchronous fluorescence scan

Introduction

Resonance Rayleigh scattering (RRS) is based on the elastic photon scattering occurring close to, or at photon absorption wavelengths [1]. Resonance Rayleigh scattering means that when exciting the sample, not only the transmission and reflection exist but coherent emission in other directions as well are present [2]. Hence, existing RRS measurements verify that the fluorophore's resonance synchronous fluorescence spectrum at zero wavelength interval ($\Delta\lambda = 0$ nm), this synchronous fluorescence spectrum at $\Delta\lambda = 0$ nm is the same as the RRS spectrum [1]. The mechanism of RRS includes the electronic polarizability of the sample molecule, where the polarizability is the measure of the charge distribution and its shift during electromagnetic radiation [3]. RRS is affected initially by the energy level transitions of the electrons and by the forced vibration caused by the electromagnetic effect of the incident light in the molecule [4]. The intensity of the RRS radiation increases remarkably as the ratio of particle size to wavelength increases. Hence, the RRS intensity is related to the aggregation diameter according to the below equation [5]:

$$\frac{I2}{I1} = a_{rel}^3$$

where I_2 is the scattering intensity of the aggregated nanoparticles – analyte, I_1 the scattering intensity of the analyte, and a_{rel} is the relative diameter of particles; $a_{rel} = a_2/a_1$ where a_1 and a_2 are the relative diameter of the particle before and after adding nanoparticles. This technique is very sensitive to several interactions as intermolecular electrostatic attraction, hydrogen bonding, hydrophobic interaction and the aggregation interaction of the molecules [6].

RRS technique can contribute to new information regarding the molecular structure and the composition, size, shape, charge distribution and refractive index of the medium [3, 7]. Because detection limit obtained in RRS is lowered by several orders of magnitude when it is compared with other spectroscopic techniques, RRS technique is therefore used to sensitively determine molecules. However, RRS technique is usually related to the use of nanoparticles as probes to detect several analytes. In fact, researchers have developed many

✉ Digambara Patra
dp03@aub.edu.lb

[1] Department of Chemistry, American University of Beirut, Box 11-0236, Riad El Solh, Beirut, PO 1107 2020, Lebanon

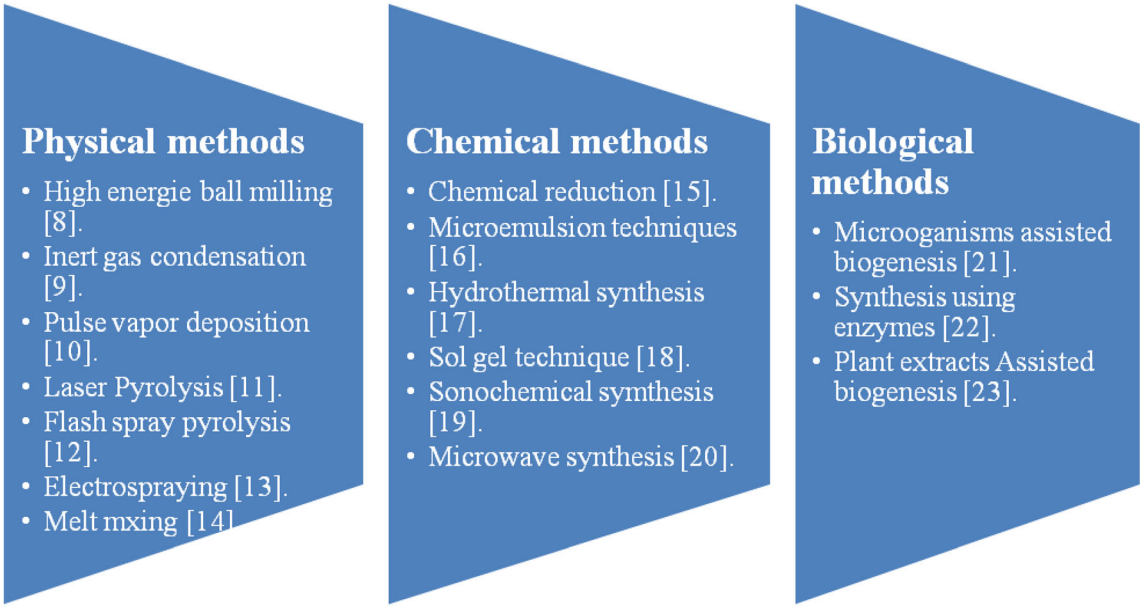

Fig. 1 Different synthesis routes to produce nanoparticles

synthesis techniques to produce nanoparticles including physical [8–14], chemical [15–20] and biological [21–23] methods (See Fig. 1).

Chemical methods are relatively the most used in the nanoparticles synthesis field, specifically the reduction method which is easy to manipulate, low cost experiment and conduct to the formation of several shapes nanoparticles using simple synthesis route. The chemical reduction method requires the use of reducing agent as sodium borohydride, CTAB, polymers, etc. with or without stabilizing agent [24]. Briefly, the formation of the nanoparticles is induced when adding the reducing agent, the metal M^{x+} go throuagh 6 steps until it turned to M^0 and precipitate as nanoparticles. It starts with the deprotonation of the reducing agent, reduction, nucleation, growth, cleavage, and ends with the maturation of the nanoparticles [25]. The mechanism of the chemical reduction method is resumed in Fig. 2. The nanoparticles formed are shown in rod shape. Hence, it is necessary to mention that different shapes of nanoparticles can be formed as spheres, wires, hexagonal, etc. The difference in shape is affected by the starting material and the experiment conditions.

Nanoparticles were extensively used in detecting different analytes such as proteins, metal ions, environment pollutants, etc. Nowadays, researchers tend to develop RRS method in the purpose of detecting several molecules using nanoparticles as probes. In general, when adding the probe to the tested analytes two different cases can exit either the RRS intensity decreases due to the fact that the nanoparticles dissociate and come apart, or the RRS intensity increases due to the increase in the size and the aggregation of the nanoparticles (See Fig. 3).

In general, gold and silver nanoparticles are mostly used as nanoprobes. However, cadmium [26] and cobalt nanoparticles [27] are also being developed in few cases as nanoprobe to determine several analytes using RRS technique. To our knowledge no review has appeared on this topic for analytical and sensing application, therefore, in this review we discuss the importance of RRS technique in sensing different analytes using gold and silver nanoparticles as probe.

Sensing using gold nanoparticles

Gold nanoparticles are widely used and developed in nanotechnology due to their unique physical and chemical characteristics, optoelectronic properties, large surface-to-volume ratio, excellent biocompatibility, and low toxicity [28, 29]. Gold nanoparticle probes are widely used in different field mainly in biomedical application starting with the determination of oligonucleotides [30], polynucleotides [31], DNA [32] and proteins [33]. Recently, they were developed to be used in analytical chemistry in the purpose of detecting metal ions [34, 35]. However, all these applications are usually applied using absorption or fluorescence spectrum, calorimetric determination or electrochemical technique. As RRS technique was found to be easier and faster, researchers have developed the determination of several analytes and proteins using resonance Rayleigh scattering.

Determination of proteins

Negatively charged gold nanoparticles can react with positively charged proteins through electrostatic force, or hydrogen bond or hydrophobic effects inducing the aggregation of the nanoparticles, thus the change in the RRS signal.

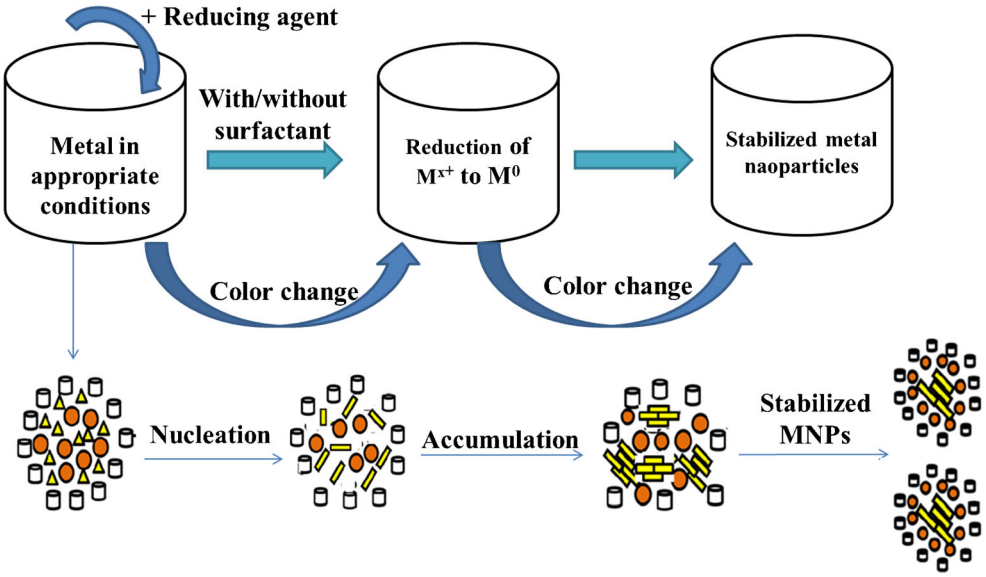

Fig. 2 Simplified scheme for the preparation of metal nanoparticles

Determination of serum albumin, bovine serum albumin and ovalbumin

Liu et al. [36] have reported the determination of three positively charged proteins (Au NPs Ova-HAS-BSA) such as serum albumin (HSA), bovine serum albumin (BSA) and ovalbumin (Ova) using gold nanoparticles. Au NPs have been synthesized according to the sodium citrate reduction, in order to obtain Au NPs solution with a concentration equal to 47.8 $\mu g.mL^{-1}$. The Au NPs were 12 nm in size with maximum scattering wavelength located at 287 nm. In fact, the three proteins HSA, BSA and Ova have very weak RRS signal. The fact of adding HSA on Au NPs solution increased the size till 23 nm inducing the aggregation of the particles. However, Au NPs mixed with HSA solution had higher RRS intensity compared to Au NPs-BSA and Au NPs-Ova. However, the difference in the intensity between the protein alone and the mixture of Au NPs-protein is due to the formation of binding product resulting in the appearing of new RRS spectra. Consequently, Au NPs with different concentration of HSA were analyzed using RRS technique. Hence, when increasing the concentration of HSA from 0.1 $\mu g.mL^{-1}$ to 0.25 $\mu g.mL^{-1}$ the RRS intensity increased with a red shift of the peak from 287 nm to 303 nm. In fact, when Au NPs binds with the proteins similar spectral characteristics appear, where the maximum wavelengths are red shifted to 303 or 304 nm from 278 nm with two new scattering peaks at 367 and 500 nm. However, the enhancement in the resonance is mainly due to the fact of the RRS spectrum of the binding product is located near the absorption band. Hence, the scattering can resonate with the light absorption and consequently it will produce a resonance Rayleigh scattering inducing the enhancement of the scattering intensity. Although, the increasing of HSA, BSA or Ova will affect the size of the Au NPs inducing the aggregation of the nanoparticles in the solution and therefore the scattering intensity increases. Mainly, the positively charged proteins when adsorb on the negatively charged gold nanoparticles surface, the electric charges are neutralized where the hydrophobic group is exposed. Therefore, the hydrophobicity of the mixture increases and in consequence the scattering intensities increases also. Hence, Liu et al. have

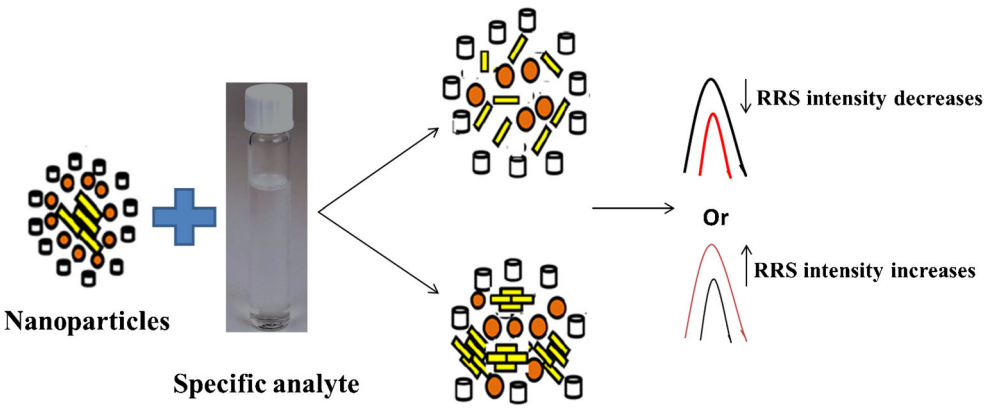

Fig. 3 Change in the RRS intensity when mixing the nanoparticles with the specific analyte

verified the efficiency of the RRS method to detect HSA, BSA and Ova in the linear range between 0.0013–0.45 μg.mL^{-1}, 0.0015–0.35 μg.mL^{-1} and 0.0019–0.40 μg.mL^{-1} respectively. In addition, the detection limits were 0.38 ng.mL^{-1}, 0.45 ng.mL^{-1} and 0.56 ng.mL^{-1} for HSA, BSA and Ova respectively. Finally, in order to study the selectivity of the described method the Au NPs-HSA system was used as an example and it was found that no interference is occurred and coexist when detecting some amino-acid, metal ions, nonmetal ions and saccharides. In conclusion, Liu et al. were able to demonstrate the specificity and efficiency of the RRS method in the purpose of proteins sensing in low concentration range. It is good to mention that Zhu et al. were able to detect Ova, HSA and BSA using cadmium sulphide nanoparticles (CdS NPs) and RRS technique. In this case the detection limit were found to be 18.5 ng.mL^{-1}, 16.7 ng.mL^{-1} and 19.6 ng.mL^{-1}respectively. Despite that the value obtained using CdS NPs are higher than the one obtained using Au NPS as probes, the use of nanoparticles to detect proteins molecules based on RRS technique give better results in comparison with other method as shown in Table 1. However, RRS methods is not useful in the higher concentration ranges and molecular interaction from other protein molecules with Au NPs can be a challenge.

Determination of glycoproteins

Folate receptors (FRs) are one the glycoproteins family present on cell membrane [42]. In general, the determination of FRs is established using fluorescence quenching or imaging, etc. where it is necessary to use fluorescent dyes and expensive instruments [43, 44]. Wu et al. [45] have succeeded in developing RRS technique method to detect FRs in serum sample using modified surface gold nanoparticles using Anti-FRα. In fact, the intensity of the RRS signal of antibody modified Au NPs is slightly higher than the intensity of Au NPs alone, which was expected since the surface of the Au NPs was changed after modifying it with anti-Frα antibody. Excitingly, when adding Frα the RRS intensity increased, which is due to the interaction between Frα and anti-Frα present on the surface of the Au NPs. Hence, the RRS intensity enhanced gradually when increasing the concentration of Frα from 2.50 to 37.50 ng.mL^{-1}. This enhancement is attributed to the dramatic aggregation of Au NPs when adding FRα caused within the interaction between anti-FRα antibody on the surface of Au NPs and FRα. Therefore, the selectivity of the RRS technique was established by analyzing the impact of coexisting substances such as saccharides, proteins, amino acids and metal ions, where it was found that these compounds would not affect the determination of Frα. Generally, there is no doubt concerning the selectivity of the described method, since anti-FRα present on the Au NPs surface will only recognize FRα. Finally, the recovery of standard addition in diluted human serum was done to evaluate the accuracy and the feasibility of the RRS technique to detect FRα. It was found that the recovery was between 90.88% and 105.59% which reveal the accuracy of the method to determine FRα in serum. In this contribution, Wu et al. have demonstrated the efficiency of RRS technique using modified Au NPs to detect Frα in the range between 2.50–37.50 ng.mL^{-1}, with detection limit equal to 0.05 ng.mL^{-1}. The difference between other reported method and the RRS technique in detecting traces of Frα is summarized in Table 2. RRS method could achieve lower LOD but the linear dynamic range is limited compared to fluorescence method.

Determination of iron binding-proteins

Human Holotransferrin (TF), a type on iron-binding proteins which is the principal iron transport of blood circulation [48]. The most common methods used to detect TF are enzyme linked immunosrbent assay ELISA [49] and electrode based immunosensor [50], which are time consuming with poor reproducibility. Therefore, Cai et al. [51] have reported RRS technique method to detect TF based on anti-TF-conjugated nanoprobe as a prototype. For this purpose, antibody conjugated nanoprobe were formed by modifying the surface of Au NPs using cysteamine and conjugating the amine functional surface with anti-TF antibody. To evaluate the feasibility and sensitivity of RRS for immunoassay through nanoprobes, the RRS intensity was measured at each step when preparing anti-TF conjugated Au NPs. It was verified, that when adding first

Table 1 Comparison of the RRS technique in detecting serum albumin and bovine serum albumin with other analytical method

HSA	Methods	LOD	Concentration Range
	High-performance liquid chromatography [37]	0.128 mg.mL^{-1}	0.4–25 mg.mL^{-1}
	Emission fluorescence using Poly(Thymine)-Templated Cu NPs [38]	5.45 mg.mL^{-1}	9–150 mg.mL^{-1}
	RP- High-performance liquid chromatography [39]	0.2 mg.mL^{-1}	0.2–20 mg.mL^{-1}
	RRS technique based on CdS NPs [26]	16.7 ng.mL^{-1}	0.065–5 μg.mL^{-1}
	Using RRS method based on Au NPS [36]	0.38 ng.mL^{-1}	13–450 ng.mL^{-1}L
BSA	Highly sensitive ELISA technique [40]	0.38 μg.mL^{-1}	0.5–40 μg.mL^{-1}
	A reversed-phase high-performance liquid chromatography [41]	0.5 μg.mL^{-1}	1–100 μg.mL^{-1}
	RRS technique based on CdS NPs [26]	19.6 ng.mL^{-1}	0.056–4.5 μg.mL^{-1}
	Using RRS method based on Au NPs [36]	0.45 ng.mL^{-1}	1.5-350 ng.mL^{-1}

Table 2 Comparison of the RRS technique in detecting folate receptors with various methods

Methods	LOD	Concentration Range
Fluorescence imaging [44]	20 $ng.mL^{-1}$	120–2000 $ng.mL^{-1}$
Electrochemical technique [46]	4.57 $ng.mL^{-1}$	25.08–1000 $ng.mL^{-1}$
Colorimetric analysis [47]	0.46 $ng.mL^{-1}$	1–100 $ng.mL^{-1}$
RRS technique based on anti-Frα modified Au NPs [45]	0.05 $ng.mL^{-1}$	2.5-37.5 $ng.mL^{-1}$

cysteamine the RRS intensity is higher than the RRS intensity of Au NPs alone. Therefore, the RRS increase respectively when adding anti-TF to cysteamine and after adding TF to the mixture. In consequence, anti-TF conjugated Au NPs can amplify the determination of TF antigen. To estimate the efficiency of the RRS technique using modified Au NPs at low concentration, the RRS intensity of TF in solution was measured with/without nanoprobe. In fact, when adding TF to the solution containing anti-TF modified Au NPs, at different concentration in the range between 85 pM-3.4 nM, a linear increase was observed. This is attributed to the fact that TF are connected to the antibody-TF present on the surface of Au NPs. However, in absence of nanoprobe, the linear increasing started from a concentration higher than 0.7 nM which indicate the low detection limit that the modified Au NPs can help in detecting TF. Hence, the increase in the RRS signal is attributed to the signal amplification and the specific recognition of nanoprobes. In consequences, the immobilized anti-TF present on the Au NPs surface can easily bind to the TF antigen and therefore resulting in the aggregation of the Au NPs which will induce the increasing of the RRS intensity. Furthermore, to study the selectivity of this method, substances and salt that can interfere with TF were analyzed and no interference was obtained. In addition, the reliability and applicability of the method, diluted human serum were collected and measured the TF concentration. The % of recovery was between 98.7% and 104%, and the calculated concentration was in correlation with the clinical data. After all, Cai et al. were able to demonstrate and to develop the RRS technique in order to detect traces of TF in the range of concentration between 85 pM and 3.4 nM, with a limit of detection equal to 85 pM. Table 3 clarifies the difference between the ELISA and electrode immunosensor method. ELISA and electrode immunosensor perform and provide better LOD compared to RRS technique.

Table 3 Comparison of the RRS technique in detecting Human Holotransferrin with ELISA and electrochemical method

Methods	LOD	Concentration Range
ELISA technique [49]	0.01 nM	0.01–2 nM
Electrode immunosensor [50]	0.019 nM	0.019–100 nM
RRS technique [51]	85 pM	85 pm-3.4 nM

Determination of G proteins-coupled receptors (G-PCR)

G protein-coupled receptors are the main promising target proteins in drug delivery research. In fact, the β-adrenergic receptors are the most important prototype in the G-PCR family, regarding there structure and regulation [52]. Salmeterol Xinafoate, one of the β-adrenergic receptors family, is a long acting and highly selective β2 agonist formulated as its 1-hydroxy-2-napthoate (xinafoate) salt used in the treatment of long-term asthma and chronic obstructive pulmonary disease [53]. To be able to detect salmeterol using simple and fast technique, for this purpose Bi et al. [54] have developed the RRS technique. It was found that the RRS intensity is higher for Au NPs - Salmeterol Xinafoate compared to Au NPs alone or Salmeterol Xinafoate alone. However, when increasing the concentration of Salmeterol Xinafoate added to the Au NPs solution the RRS intensity enhanced indicating that the particles increased in size. The increasing in the particle size is due to the interaction of Au NPs with Salmeterol Xinafoate. In fact, the anionic species of Salmeterol Xinafoate interact easily with the positively charged Au NPs through electrostatic adsorption inducing the aggregation of Au NPs - Salmeterol Xinafoate and the formation of larger particles, enhancing thereby the RRS intensity. In addition, the selectivity of the method was carried out within testing foreign substances with positive or negative charge as cations and glucose. It was found that these samples have no influence on the RRS intensity when mixed with Au NPs verifying the selectivity of the developed method. Finally, the recovery of the method analyzing synthetic sample was estimated to be around 102.5–103% which reveals the accuracy, precision, reliability and selectivity. To conclude, Bi et al. have reported new RRS technique to detect Salmeterol Xinafoate using Au NPs in the concentration range between 0.054–6.038 $\mu g.mL^{-1}$, with low detection limit equal to 9.48 $ng.mL^{-1}$. Many analytical methods used to determine salmeterol xinafoate are expensive, time consuming and possesses poor repeatability. And yet, these methods cannot detect salmeterol xinafoate in very low concentration with a low detection limit as good as that of RRS. The difference is illustrated in Table 4. Though RRS technique provides a better LOD it fails in higher concentration where HPLC and spectrophotometric methods perform well.

Table 4 Efficiency of the RRS technique in detecting Salmeterol Xinafoate compared to other methods

Methods	LOD	Concentration Range
Reverse phase high performance liquid chromatography [55]	0.260 $\mu g.mL^{-1}$	2–49.3 $\mu g.mL^{-1}$
Spectrophotometric method [56]	0.022 $\mu g.mL^{-1}$	12–60 $\mu g.mL^{-1}$
RRS technique [54]	9.48 $ng.mL^{-1}$	0.054–6.038 $\mu g.mL^{-1}$

Determination of transmembrane proteins

The epidermal growth factor receptor (EGFR) is a transmembrane protein, considered as a receptor for members of the epidermal growth factor family of extracellular protein ligands [57]. Li et al. [58] have described the conjugation of the Au NPs to the anti-EGFR aptamer (Apt) in order to determine the EGFR through RRS method. In fact, the thiol modified Apt were conjugated to the surface of Au NPs through Au-S bond to obtain the Apt-Au NPs probe. Hence, when adding EGFR, it will bind anti-EGFR as shown in Fig. 4. This contributes to the formation of a binding complex which is the Apt-AuNPs–EGFR.

The formation of the complex is verified by the change of color from red to blue increasing the RRS intensity of the Apt-Au NPs alone. Consequently, the addition of EGFR at different concentration attribute to the aggregation of the probe around the EGFR protein, therefore the formation of bigger EGFR-Apt-Au NPs particle inducing the increase of the RRS intensity. The enhancement of the RRS intensity was proportional to the EGFR concentration in the range between 30 and 110 $ng.mL^{-1}$. The change in the intensity is the reason of the binding between the Apt-Au NPs probe and EGFR through specific recognition which leads to the assembly of the probe around the EGFR. Thus, the binding products were enlarged in volume which is the principal reason to increase the RRS intensity. Hence, the hydrophobicity of the binding products increased and a liquid-solid interface between the complex and water may be formed enhancing thereby the scattering intensity. The selectivity of the formed Apt-Au NPS probe was verified where no change in the RRS intensity was mention when mixing the probe with bovine serum albumin, vascular endothelial growth factor and PDGF. Finally, the accuracy of the method was estimated by measuring the EGFR concentration in human serum sample without any complicated pre-treatment. However, the calculated concentrations according to the RRS technique were almost the same as the concentrations calculated from the laboratory data. Based on the above data, Li et al. have verified the simplicity and the rapidity to recognize the EGFR in human serum using RRS technique in comparison with other analytical methods these methods require several steps and are not strictly quantitative. Therefore, they have low sensitivity and high cost of apparatus. Some examples of other method to detect EGFR are mentioned in Table 5. Microfluidic immunosensor performs better in lower concentration compared to RRS method.

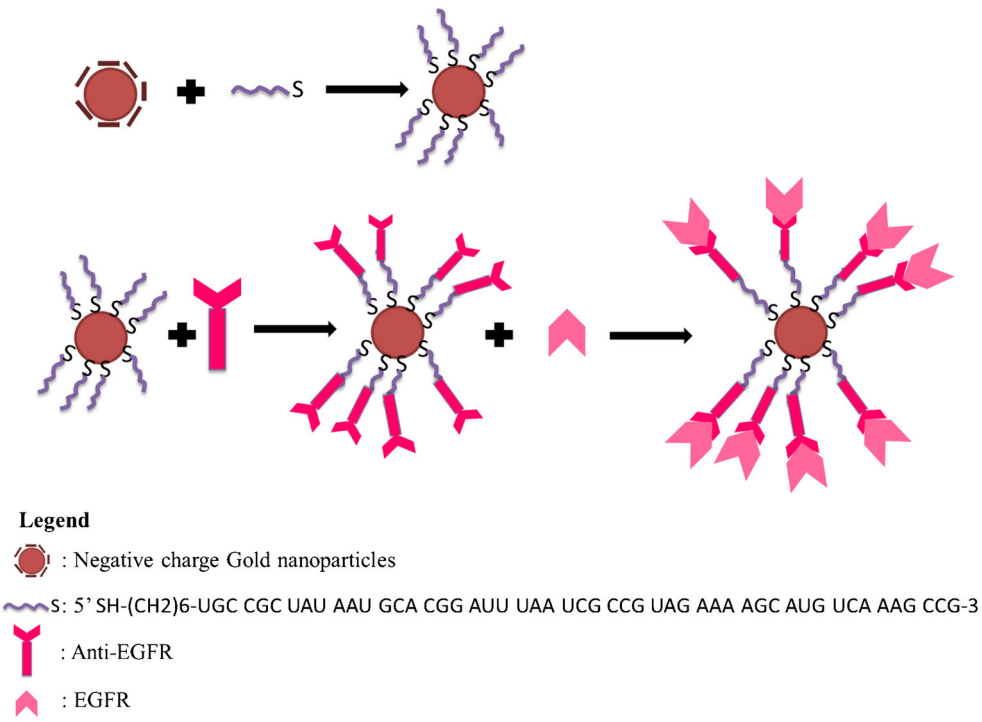

Fig. 4 Specific recognition of EGFR proteins through anti-EGFR antibody

Table 5 Comparison of the selectivity of RRS technique in detecting epidermal growth factor receptor to several methods

Methods	LOD	Concentration Range
Quartz crystal microbalance [59]	100 ng.mL^{-1}	10–10,000 ng.mL^{-1}
Electrochemical technique [60]	50 pg.mL^{-1}	1–40 ng.mL^{-1}
Microfluidic immunosensor [61]	3.03 pg.mL^{-1}	0.01–50 ng.mL^{-1}
RRS technique [58]	0.7 ng.mL^{-1}	0.03-0.11 g.mL^{-1}

Determination of cysteine

Aggregation of Au NPs can be achieved by adding cysteine [62]. In this case Au NPs will self-assemble to form a network structure and enhance greatly RRS signal within the increasing of the cysteine concentration. Therefore, RRS technique has been applied by Li et al. [63] to selectively determine cysteine with high sensitivity and simple operation. The linear range of determination of cysteine is from 0.01 to 0.25 microg/mL with the detection limit of 2.0 ng/mL (16.5 nM, 3sigma). None of the amino acids found in proteins interferes with the determination. The difference between the available method and the RRS technique is resumed in Table 6.

Determination of sulfur fungicides

The application of pesticides and fungicides to protect and increase the yield of agricultural product is one of the major public health. Thiram (THM) is a type of sulfur fungicides used in sun screen and as a bactericide applied directly to the skin or incorporated into soap. Therefore, it is vital to establish sensitive and effective method to detect THM. Parham et al. [66] have developed the use of Au NPs as an optical probe to detect THM by measuring the RRS intensity. However, they have observed the change in the size and shape of Au NPs when adding THM, where the Au NPs-THM complexes have bigger size which will enhance the RRS intensity of Au NPs. It is good to mention that the interaction between Au NPs and THM is assumed by the sulfur group in THM that will self-assemble into strictly arranged monolayers and contribute to the formation of A-Au bond. THM alone possesses weak RRS almost negligible, in contrast when adding THM to Au NPs solution the RRS intensity of the solution increases.

Table 6 Comparison of the selectivity of RRS technique in detecting cysteine with available method

Methods	LOD	Concentration Range
Electrochemical method [64]	5 μM.L^{-1}	5–1000 μM.L^{-1}
Calorimetric technique [65]	0.05 μM.L^{-1}	1.5–6 μM.L^{-1}
RRS technique [63]	16.5 nM.L^{-1}	0.08–2 μM.L^{-1}

The addition of THM was carried out regarding 2 different ranges from 1 to 30 and 30–200 μg.L^{-1}. It was found that upon the addition of THM the RRS intensity of Au NPs increases and the results show low detection limits equal to 0.3 μg.L^{-1}. The intra- and inter-day precision and accuracy data were established by measuring the RRS determination of THM in quality controlled (QC) water samples. It was found that the results conform to the criteria of the water analysis samples according to the guidance of US-FDA. Hence, the recovery values from (QC) water sample containing different concentrations were quite acceptable between 96 and 111%. Finally, the validation of the method was verified within the determination of THM in water and plant sample. It can be concluded that Parham et al. have successfully developed the RRS technique in the purpose of the determination of ultra-traces of THM. This method will be applicable to determine the concentration of THM in water and plant sample with low detection limit compared to different analytical method (See Table 7. However, binding of Au NPs with other analyte can be a challenge in RRS method.

Determination of saccharides

Saccharides are considered as organic compounds extracted from non-sea vegetables that include sugars. However, glucose is the most important sugar in human metabolism [70]. El-Kurdi et al. [25] have demonstrate the capability of detecting glucose using RRS technique based on gold nanoparticles as probe. In this study, Au NPs were synthesized regarding a green synthesis method using curcumin as reducing agent and F-108 polymer as stabilizing agent. The determination of glucose molecule was established in a very wide range between 0 and 10 mM with same concentration of Au NPs. The fact of adding glucose to the Au NPs solution had a significant effect on the RRS signal of Au NPs. Therefore, when increasing the concentration of glucose, about~8 fold increase in the RRS intensity was recorded without any change in the spectral shape and RRS wavelength maximum (See Fig. 5). This boost in the intensity is due to the adsorption of glucose molecule on the surface of the nanoparticles since Au NPs possesses large surface area and high surface free energy.

However, RRS intensity increasing is also related to the particle size and its aggregation in the solution. In fact, F-108 polymer present in the system to stabilize the Au NPs binds competitively with the glucose molecule and promotes the formation of large aggregates on the surface of Au NPs which boost the RRS intensity. Furthermore, the efficiency of the tested method was confirmed by detecting glucose molecule using Au NPs in the presence of boric acid or glucose oxidase. However, boric acid contains hydrogels that allows them to exhibit interesting properties such as glucose selectivity/sensitivity and glucose oxidase is an oxidoreductase that improves the oxidation of glucose and therefore its determination. Hence, it has been verified that Au NPs can act as immobilization enzyme matrix and in

Table 7 Comparison of the RRS technique in detecting Thiram with other analytical method

Methods	LOD	Concentration Range
Solid phase micro-extraction-high pressure liquid chromatography [67]	1 $\mu g.L^{-1}$	1–10 $\mu g.L^{-1}$
Solid phase extraction-UV [68]	10.8 $\mu g.L^{-1}$	25–175 $\mu g.L^{-1}$
Adsorptive stripping voltammetry [69]	9.8 $\mu g.L^{-1}$	20–150 $\mu g.L^{-1}$
RRS technique [66]	0.3 $\mu g.L^{-1}$	1–30 $\mu g.L^{-1}$
		30–200 $\mu g.L^{-1}$

consequences enhance the activity between the nanoparticles and glucose molecule. The above described method was also useful to detect glucose in human serum where several solutions were prepared by spiking serum with known glucose concentration in the range between 0 and 10 mM. Hence, El-Kurdi et al. have demonstrated the efficiency of the RRS technique in order to detect glucose molecule with a LOD = 20 μM. Finally, to test the selectivity of the methods, other potential anti-oxidant interferences were tested, and it was noticed that no interference was occurred with the glucose determination. To sum up, El-Kurdi et al. have proven the selectivity and the specificity of the resonance Rayleigh scattering technique to detect glucose molecule using gold nanoparticles as probe. Table 8 summarizes the efficiency of the above method in glucose determination in the large range between 0 and 10 mM with any additional enzyme, compared to other technique, however, RRS method many not be applicable to estimate glucose in lower concentration range found in food and beverages.

Determination of vitamins

Determination of α-tocopherol

A vitamin is relatively an organic molecule with low molecular weight, essential micronutrient that an organism needs for the proper functioning of its metabolism and normal growth. α-Tocopherol is the most important group of the tocopherols and known as vitamin E. α-Tocopherol possesses several functions and natural phenolic anti-oxidant properties, where it prevents the oxidation of lipids that would ensure the establishment of undesirable compounds producing oil deterioration. El-Kurdi et al. [74] have succeeded to develop RRS technique measurement in order to detect α-Tocopherol based on Au NPs probe, synthesized using curcumin and cetyltrimethylammonium bromide. Interestingly, when adding α-Tocopherol to the Au NWs solution, the RRS signal of Au NPs increases about ~ 10-fold, with the increase of the α-Tocopherol concentration in the range between 12.8–1004 $\mu M.L^{-1}$ (See Fig. 6). However, the boost in the RRS signal did not alter the wavelength maximum and the shape of the spectra.

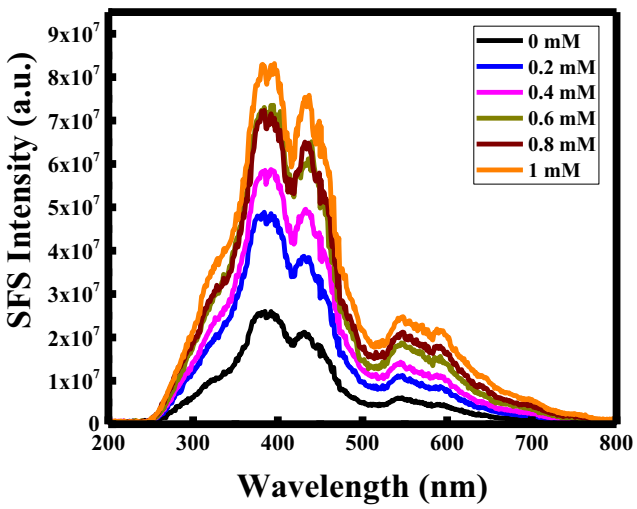

Fig. 5 **a** Synchronous fluorescence spectra (SFS) at Δλ = 0 nm of curcumin functionalized Au NPs with different concentration of glucose

Hence, the fact of adding α-Tocopherol to the Au NWs improve the complexation of α-Tocopherol with the nanowires through non-covalent interaction and thereby the formation of larger complex, which induce the change in the intensity of RRS signal. This interaction is most likely facilitated by the presence of curcumin conjugation at the surface of Au NWs through hydrophobic interaction. Furthermore, to test the selectivity of the method, different potential anti-oxidant that can interfere with α-Tocopherol as ascorbic acid and 6-O-palmitoyl ascorbic acid were tested. It was found that for 30 $\mu M.L^{-1}$ for each analyte with Au NWs did not alter the RRS signal of Au NWs unlike ~9 fold increase observed for same concentration of α-Tocopherol. Finally, the method applicability was established by preparing synthetic samples of α-Tocopherol and estimating the concentrations using the calibration plot where the % recovery was between 92%–98% indicating the good applicability of the presented method. Therefore, El-Kurdi et al. have verified the selectivity of the RRS technique to detect α-Tocopherol in the large range between 12.8–1004 $\mu M.L^{-1}$, with very low detection limit equal to 50 $nM.L^{-1}$. In general, most of the available methods for α-Tocopherol sensing reveal low concentration range. The difference between the above method and the available on in the literature is resumed in Table 9. The major challenge for RRS technique here could be real sample analysis, where it may necessitate a separation procedure.

Table 8 The effectiveness of RRS method in glucose sensing compared to other method

Methods	LOD	Concentration Range
Colorimetric assay based on MnO2 Nano-sheets combined to glucose oxidase [71]	12.8 $\mu M.L^{-1}$	0–100 $\mu M.L^{-1}$
Electrochemical method based on GOD incorporated intou Au-CNT electrode [72]	17 $\mu M.L^{-1}$	0.05–1 $mM.L^{-1}$
Liquid Chromatography method [73]	100 $\mu M.L^{-1}$	0.01–0.5 $mM.L^{-1}$
RRS technique based on Au NPs probe [25]	20 $\mu M.L^{-1}$	0.2-10 $M.L^{-1}$

Determination of thiamine

Thiamine also called vitamin B1, is present in many food product as yeast, beans, nuts, etc. [78]. Liu et al. [79] have used gold nanoparticles in the determination of thiamine. Liu et al. have verified that vitamin B1 can interact with Au NPs inducing the formation of a binding product. Hence, the formed complex enhances the resonance Rayleigh scattering intensity. The increasing of the RRS intensity was proportional to the increasing in the concentration of vitamin B1 in the range of 0–270 $nM.L^{-1}$with a detection limit equal to 0.9 $ng.mL^{-1}$. However, the formed Au NPs were negatively charged due to the adsorption of the citrate molecule on the surface of the nanoparticles. Hence, supramolecular compound with negative charge is formed and thereby it can react with vitamin B1 through electrostatic interaction. Therefore, the RRS intensity increases with the appearance of new RRS peaks. It was found that the RRS intensity for the final product obtained remains constant in 50 min. Finally, the concentration of vitamin B1 was calculated in 20 tablets and it was remarkable that the concentration found according to the RRS technique were similar to the clinical data value. In general, RRS technique in the purpose of the determination of vitamin B1 can be used to calculate the concentration in tablets and it's not applicable to complex matrix such as food samples. The difference in the detection limit between the RRS technique and other methods is presented in Table 10. But emission analysis still found to be a better alternative with lower LOD.

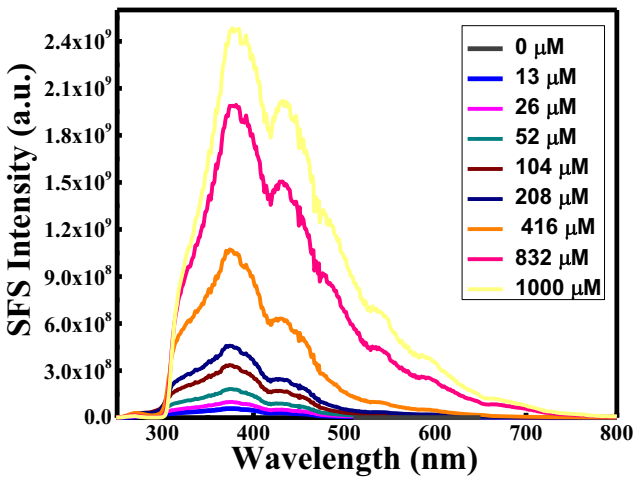

Fig. 6 Synchronous fluorescence spectra (SFS) at $\Delta\lambda = 0$ nm of curcumin conjugated Au NWs with different concentration of α-tocopherol

Determination of heavy metal pollutant

Heavy metals are metallic elements that denser than water. Heavy metals are also considered as trace elements because of their presence in trace concentrations less than 10 ppm in various environmental matrices. Such of these metals includes mercury, silver and chromium [83].

Determination of mercury ions

Mercury is a highly toxic heavy metal element that is distributed in nature. Hence, it is necessary to develop cheap and sensitive method in the purpose of its determination. Ouyang et al. [84] and Gao et al. [85] have evaluated the RRS technique based on Au NPs with and without modification to detect traces of Hg^{2+} in water sample. In fact, in 2014 and for the first time Gao et al. were able to detect Hg^{2+} using double standard DNA modified nanoparticles standards (dsDNA-Au NPs). Later on, in 2017 Ouyang et al. have established the determination of Hg^{2+} using Au NPs synthesized with trisodium citrate and sodium borohydride and reading $HAuCL_4$ to the final nanoparticle solution. However, contradictive results were obtained for both studies were in the case of using (dsDNA-Au NPs) the RRS intensity of Au NPs after adding Hg^{2+} increases respectively, while in the second case where no modification of the Au NPs surface was carried out the RRS intensity decreases. Hence, in both cases the detection limit was very low where Ouyang et al. have got a LOD value equal to 3 $nM.L^{-1}$ (8–1330 $nM.L^{-1}$) and Gao et al. the LOD was equal to 0.4 $nM.L^{-1}$ (2.5–60 $nM.L^{-1}$). Although, the LOD was lower using dsDNA-Au NPs

Table 9 Comparison of the RRS technique in detecting α-tocopherol with other analytical method

Methods	LOD	Concentration Range
High performance liquid chromatography [75]	1.35 μM.L^{-1}	117–700 μM.L^{-1}
High performance liquid chromatography/Uv [76]	1.51 μM.L^{-1}	16.7–65 μM.L^{-1}
Electrochemical method [77]	0.45 μM.L^{-1}	5–200 μM.L^{-1}
RRS technique [74]	50 nM.L^{-1}	12.8-1004 μM.L^{-1}

but the concentration range was bigger in the second case. Gao et al., attribute the increasing of the RRS intensity after adding Hg^{2+} to the coordination of Hg^{2+} with T base pair. In fact, the double standard DNA possess a mismatched T-T base pair in the chain terminus which prevent the au NPs from aggregation which will leads, in the presence of Hg^{2+}, to the non-cross-linking aggregation of dsDNA-Au NPs regarding the coordination of Hg^{2+} with the T base pair where Hg^{2+} ions will be incorporated between the T-T base pair and will give T- Hg^{2+}-T. Hence, Gao et al. have been able to detect Hg^{2+} in the range between 2.5–60 nM.L^{-1} with LOD equal to 0.4 nM.L^{-1}. Therefore, Ouyang et al. have facilitated the determination method of Hg^{2+} using unmodified Au NPs through citrate reduction method. In this case, the resulted complex obtained after the addition of Hg^{2+} adsorb strongly on the negatively charge surface of Au NPs due to the presence of citrate anions and inhibits the red electron transfer and decreased consequently the catalytic reaction of the nanoparticles which leads to the decreasing of the RRS intensity of Au NPs. Accordingly, Ouyang et al. were capable to develop the RRS technique to detect Hg^{2+} in a wide concentration range 8–1330 nM.L^{-1} with LOD equal to 3 nM.L^{-1}. However, the both experiments were used to detect Hg^{2+} in water sample with a percentage recovery between 97 and 102%. Finally, no interference with other metal ions was found when testing them with the described probes which verify the selectivity of the methods concerning the Hg^{2+} determination. The low detection limit of the RRS technique compared to other detection limit is illustrated in Table 11. Binding of other metal ions during estimation can be challenge in RRS technique.

Determination of silver ions

In recent years, due to the development of human activities, the Ag^{+} presence in the environment increased interestingly. In fact, Ag^{+} present in food chain and drinking water can easily accumulate in the human body. Therefore, it will lead to cell toxicity and organ failure [89, 78]. Wen et al. [90] have established for the first time the RRS technique in order to detect traces of Ag^{+} using aptamer-modified Au NPs as probe. For this purpose, single standard DNA (ssDNA) with a sequence of 5'-CTC TCT CTT CAT TTT TCA ACA CAA CAC AC-3′ was used. It was found that a stable ssDNA-Au NPS complex without any aggregation is formed. The absence of aggregation facilitates the determination of Ag^{+} where the Ag^{+} ions will interact with the aptamer and induce the aggregation of the nanoparticles. Hence, when adding Ag^{+} to the Au NPs solution, it leads to C- Ag^{+}-C mismatches and forms a similar hairpin structure, since the ssDNA is present on the surface of the Au NPs. However, when increasing the concentration of Ag^{+} from 0.067–1.33 μM.L^{-1}, the aggregated nanoparticles increases and induces the enhancement of the RRS intensity. The determination was achieved with a detection limit equal to 0.059 μM.L^{-1}. Thereby, the authors have established the effect of Cu_2O as nanocatalyst to improve the determination of Ag^{+}. In this case, the Cu_2O inhibits the aggregation of Ag^{+} -ssDNA-Au NPs and decreases the RRS intensity of the nanoparticles. However, using this procedure the Ag^{+} ions were detected in lower concentration range 3.3–666.7 nM.L^{-1} with very low detection limit equal to 3.1 nM.L^{-1}. In

Table 10 Comparison of the RRS technique in detecting Thiamine with other analytical method

Methods	LOD	Concentration Range
Emission analysis using silica nanoparticles [80]	2 nM.L^{-1}	5–1000 nM.L^{-1}
Fluorescence technique using cadmium nanorods [81]	29.6 nM.L^{-1}	100–3000 nM.L^{-1}
UV-Visible technique using AuNPs and alkaline phosphatase [82]	54 nM.L^{-1}	150–3500 nM.L^{-1}
RRS technique [79]	3.4 nM.L^{-1}	0–270 nM.L^{-1}

Table 11 The difference in the sensitivity of various methods in detecting mercury ions compared to RRS technique

Methods	LOD	Concentration Range
Electrochemical method [86]	60 $nM.L^{-1}$	20–250 $nM.L^{-1}$
Solvent extraction followed by reversed phase HPLC [87]	0.8 $nM.L^{-1}$	10–100 $nM.L^{-1}$
HPLC/ICP-MS [88]	0.4 $nM.L^{-1}$	2.5–250 $nM.L^{-1}$
RRS technique using dsDNA-Au NPs [85]	0.4 $nM.L^{-1}$	2.5–60 $nM.L^{-1}$
RRS technique using Au NPs-$HAuCl_4$ [84]	3 $nM.L^{-1}$	8-1330 $.L^{-1}$

addition, the interference of some common metal ions with a concentration equal to 0.66 $\mu M.L^{-1}$ was investigated, and it was found that these metal ions have minim effect on the Au NPs RRS intensity, which proves the selectivity of the method. Finally, the percentage of recovery was found to be between 96.7–103.6% after calculating the concentration of Ag^{+} was calculated in water samples. Compared to other method, Chen et al. have demonstrated that RRS technique is easy to operate in a wide range of concentration and with low detection limit (See Table 12).

Determination of chromium ions

Chromium is used in metal alloys such as ceramics, stainless steel, chrome plating, etc. This metal provides a durable, highly and resistant coating. Thus, it can also be toxic to the environment and to humans. In fact, chromium can have negative effects on living systems where it can accumulate in liver, brain and heart muscle [93]. Hence, chromium III is present in some human nutrition, where high level of it bind to DNA molecule and therefor it will affect the cellular structures and damage it [94] which make important to find easy technique to detect chromium. Chen et al. [95] were able to develop RRS technique in order to detect chromium III in very low concentration using gold nanoparticles formed through citrate reduction. The fact of adding Cr^{3+} to the Au NPs solution, network-liked aggregation of nanoparticles was observed which demonstrate the ability of Cr^{3+} in inducing large scaled nanoparticles through chelating reaction. Introduction of Cr^{3+} ions onto the citrate capped Au Ns enhance interestingly the RRS intensity. The increasing of the intensity is due to the fact that carboxyl groups of citrate layer presented on the Au NPs surface were chelated with Cr^{3+} which increases the size of the nanoparticles and thereby the enhancement of the RRS intensity. The RRS intensity of Au NPs increases proportionally with the increasing of Cr^{3+} concentration from 1 to 10 pM assuming that the linear determination for Cr^{3+} was established with limit of detection equal to 1 pM. The interference analysis was done to evaluate the selectivity of the method. In this purpose several metal ions were tested in a wide concentration range from 10 to 1000 $\mu M.L^{-1}$ and it was found that no increasing in the intensity was observed for all the metal tested as the increased on Cr^{3+}. Hence, Chen et al. have demonstrated the excellent selectivity of the RRS method to detect traces of Cr^{3+} over alkali, alkaline earth and heavy transition metal ions. Some analytical techniques used to detect $Cr^{3+}$are listed in Table 13. Here association of other metal ions during estimation can be challenge in RRS technique.

Determination of lead ions

Lead is a highly poisonous metal that affect almost every organ and system in the human body. It can cause severe damage to the brain and kidneys and, ultimately, death [83]. For this reason, it was necessary to find a cheap and easy technique in order to determine its quantity. Liang et al. [98] have established a new RRS technique using couple hydride generation reaction with nanogold formation. For this purpose, Pb^{2+} ions were oxidized to Pb^{4+} using $K_2Cr_2O_7$-H_2O_2, in order to facilitate the

Table 12 Comparison of the RRS technique in detecting silver ions with other spectroscopic method

Methods	LOD	Concentration Range
Fluorescence Method [91]	32 $nM.L^{-1}$	50–70 $nM.L^{-1}$
Localized surface Plasmon resonance light scattering sensor [92]	62 $nM.L^{-1}$	0.13–1.12 $\mu M.L^{-1}$
RRS intensity	58.5 $nM.L^{-1}$	0.067–1.33 $\mu M.L^{-1}$
Nanocatalytic RRS [90]	3.1 $nM.L^{-1}$	$nM.L^{-1}$

Table 13 Comparison of the RRS technique in detecting chromium ions with other analytical method

Methods	LOD	Concentration Range
Fluorescence spectrum base CdTe quantum dots [96]	20 $nM.L^{-1}$	0.0678–3.7 $\mu M.L^{-1}$
Electrochemical technique [97]	0.1 $\mu M.L^{-1}$	0.1–10 $\mu M.L^{-1}$
RRS technique [95]	1 $pM.L^{-1}$	1-10 $M.L^{-1}$

reduction to Pb(0). However, to enhance the stability of Pb^{4+}, $K_3[Fe(CN)_6]$ was added to the solution. In fact, $NaBH_4$ was used as a reducing agent that reduces Pb^{4+} to PbH_4. The PbH_4 gas was adsorb by the Au^{3+} solution to form gold nanoparticles. The determination of Pb was recorded using RRS technique. It was found that the increasing in the Pb^{2+} concentration increased the RRS intensity. Three RRS peak were obtained at 286, 368 and 518 nm. Upon the addition of Pb^{2+} in the concentration range of 0.2 and 33.6 $\mu M.L^{-1}$, the RRS intensity at the 3 peaks increased respectively, with a detection limit equal to 70 $nM.L^{-1}$.

In addition Li et al. [99] were able to detect Pb2+ ions based on the use of gold nanoparticles catalyzed by graphene oxide. In this case, Pb ions were determined in the concentration range between 2 and 75 $nM.L^{-1}$ with a detection limit equal to 0.7 $nM.L^{-1}$. Hence, the RRS technique is useful to determine Pb ions but not at high concentration. The difference in the concentration range between RRS technique and other analytical method is presented in Table 14.

Determination of cationic dye

Cationic dyes are dissociated easily in water into positively charged ions and interact with negatively charged molecule. In fact, cationic dyes assemble on the out layer of the molecule. However, cationic dye can be determined using nanoparticle with negative charge surface. Youqiu et al. [102] have studied the interaction of Safranin T (ST) dye with the out layer of gold nanoparticles and its change on the optical and spectral properties of Au NPs. The Au NPs in this case were synthesized by tannic acid-sodium citrate reduction methods which assure the presence of citrate ions on the Au NPs surface. The Au NPs resulted were spherically shaped and well dispersed, they increased in size when adding ST from 12 nm to 16 nm without changing in the shape. When adding ST in the concentration between 1.4 $\mu mol.L^{-1}$ − 250 $\mu mol.L^{-1}$ at pH 5 the RRS wavelength red shifted and the intensity decreases gradually. Youqiu et al. have defined the RRS technique to detect ST with low detection limit equal to 1.2 $pm.L^{-1}$. The authors have described the interaction between ST and Au NPs as below. First of all, the citrate ion present in the solution at pH 5 exists mainly in the species of $(H_2L)^{2-}$ and can self-assemble on the Au NPs surface where one carboxylate oxygen in $(H_2L)^{2-}$ approaches to the Au NPs surface by virtue electrostatic attraction and the other carboxylate oxygen moves outward to modify the Au NPs surface charge and make it totally negative in the form of $[(Au)_n(H_2L)_m]^{x-}$. Therefore, the resulting complex is a negative charge supramolecule. It interacts with the positively charge dye ST through the carboxylate oxygen on the surface through hydrophobic force and charge transfer action. This interaction results in the formation of a stable three layer supermolecular compound $\{[(Au)_n(H_2L)_m]^{x-}.(R^+)\}_x$. In other words, the au NPs are the kernel, the ST is the out layer and the $(H2L)^{2-}$ is the bridge between the two components. Finally, Youqiu et al. have verified the sensitivity of RRS technique in the determination of ST compared to other spectrophotometric and analytical method with very low detection limit equal to 1.2 $pm.L^{-1}$. The difference between the methods used to detect safranine T is summarized in Table 15.

Sensing using silver nanoparticles

Silver nanoparticles (Ag NPs) are interestingly gaining popularity, where researchers are developing different strategies for optical probes and imaging techniques using Ag NPs as building blocks and labeling probes [105]. Ag NPs processes high

Table 14 Comparison of the RRS technique in detecting chromium ions with other available method

Methods	LOD	Concentration Range
Electrochemical method [100]	1 $nM.L^{-1}$	1.5–240 $nM.L^{-1}$
Strip immunusensor tecgnique [101]	10 $nM.L^{-1}$	0–300 $nM.L^{-1}$
RRS technique using couple hydride generation reaction [98]	70 $nM.L^{-1}$	0.2–33.6 $\mu M.L$-1
RRS technique using gold nanoparticles catalyzed by graphene oxide [99]	0.7 $nM.L^{-1}$	2–7 $nM.mL^{-1}$

Table 15 Low LOD value of RRS technique in detecting safranin T compared to other techniques

Methods	LOD	Concentration Range
Ionic liquid coated magnetic Core/Shell Fe_3O_4@SiO_2 nanoparticles [103]	0.1 $nM.L^{-1}$	0.3–370 $nM.L^{-1}$
CTAB sensitized fluorescence quenching [104]	0.096 $nM.L^{-1}$	0.28–11 $nM.L^{-1}$
RRS technique [102]	1.2 $pM.L^{-1}$	1.4 -250 $\mu M.L^{-1}$

extinction coefficient, sharper extinction bands and high ratio of scattering to extinction [105]. Therefore, Ag NPs are considered as promising alternative of Au NPs in many applications in the domains of medicine, microbiology and analytical chemistry [106]. These days, silver nanoparticles are being developed to be used as probes to detect several analytes based on the RRS technique instead of using electrochemical, colorimetric or analytical method.

Determination of nucleic acid

Nucleic acid contain essentially the genetic information and play an interestingly role in protein biosynthesis. They are formed by the polymerization of nucleotides and consist of two major compounds D-ribose in ribonucleic acid (RNA) and D-2-deoxyribose in deoxyribonucleic acid (DNA) [107]. El khoury et al. [108] established the efficiency of detecting DNA and RNA using RRS technique and silver nanoparticles through Al^{3+} bond. In fact, β-Diketone moiety of curcumin can chelate to cationic metal as Al^{3+}. DNA alone had no RRS intensity and when adding DNA to Ag NPs solution weak RRS peak is noticed. However, the RRS intensity of Ag NPs increases interestingly when adding DNA solution to the modified Ag NPs- Al^{3+} which assures the presence of interaction between Ag NPs- Al^{3+} and DNA. The interaction is due to the adduct of Al^{3+} with the double standard DNA through phosphate groups and base residues sites (See Fig. 7).

The change in the RRS intensity is proportional to the DNA concentration in the range from 10 to 100 $\mu g.mL^{-1}$. In consequence, large aggregates will be formed when mixing Ag NPs- Al^{3+} with DNA producing Ag NPs- Al^{3+}-DNA complex, inducing the enhancement of the RRS intensity.

Subsequently, when replacing DNA molecule with RNA molecule, same results were obtained since DNA and RNA possess alternatively same structure containing phosphate groups as shown in Fig. 8. The determination of DNA and RNA was established in the concentration range between 10 and 100 $\mu g.mL^{-1}$.

Even though, that in the literature there is some technique that possesses lower LOD (See Table 16) but El-Koury et al. were able to detect DNA and RNA molecule in a very wide range between 10 and 100 $\mu g.mL^{-1}$ with very low detection limit equal to 12 and 38 $\mu g.mL^{-1}$based on RRS technique cheaper and easy to manipulate. However, electrochemical method promises to be more accurate and sensitive method in lower concentration range compared to RRS technique.

Determination of insecticides

Insecticides are protective compounds in agricultural crop against damaging caused by the insects, consist of triphosphoryl (P=S) functional group. Ethion is an organophosphate insecticide and it affects a neural enzyme called acetylcholinesterase and prevents it from working inducing the accumulation of acetylcholine at nerve endings in the peripheral; or central nervous system [113]. Parham et al. [114] have succeeded to develop the RRS technique based on the use of silver nanoparticles to detect ethion. The synthesized Ag NPs were spheres in shape and small in size about 20 nm. However, when adding ethion the particles aggregated to form bigger particles. This aggregation is due to self-assemble of the thiol groups present in the ethion molecule with the O- of the citrate group as below:

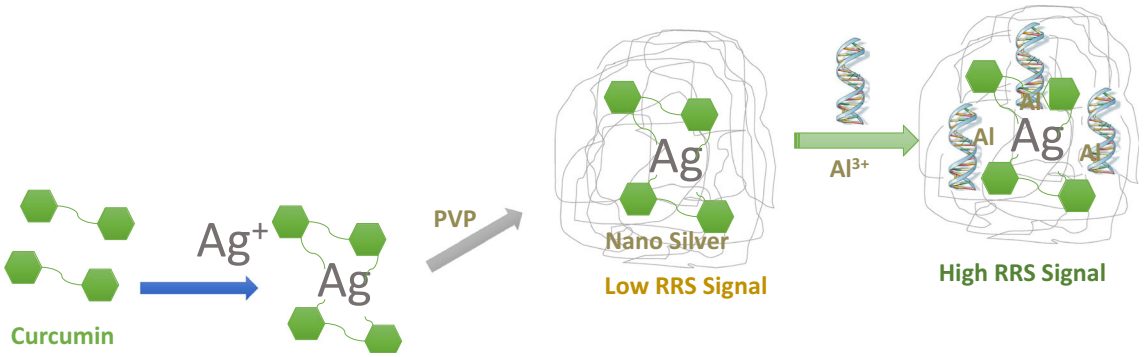

Fig. 7 Determination of DNA and RNA using Ag NPs-Al^{3+}

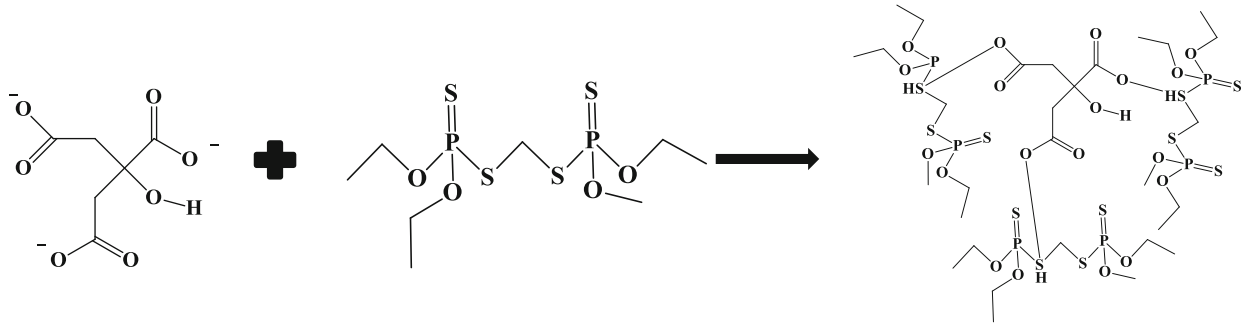

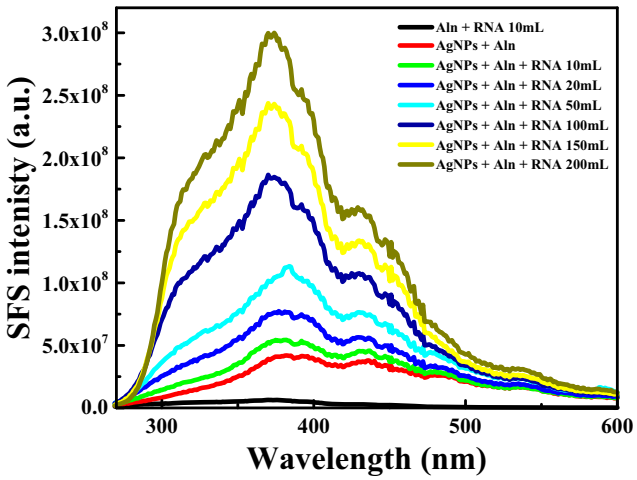

Fig. 8 Synchronous fluorescence spectra (SFS) at $\Delta\lambda = 0$ nm of Ag NPs with different concentration of RNA

This self-assemble lead to the formation of strictly arranged monolayers at high concentration, onto the surface of silver nanoparticles (See Fig. 9). This aggregation will lead to the quenching of the RRS intensity of Ag NPs after the addition of ethion.

The determination of ethion was done by adding different concentration in the region between 10 and 900 μg/L. The increasing in the concentration quenched greatly the RRS spectra, where the RRS intensity of Ag NPs decreased gradually. The detection limit was very low and equal to 3.7 μg/L. the intra and inter-day precision was also established in quality control water and in water sample.

The percentage recovery was found to be between 92 and 107%. Finally, the possibility of the interference with coexisting substances was evaluated and it was found that no interference occurred while detecting ethion molecule. Thereby, Parham et al. were able to develop the RRS technique and to prove its selectivity precision and accuracy according to the guidance of US-FDA. In addition, the detection limit was very low with a wide range of concentration in comparison with other technique as summarize in Table 17. Nevertheless, RRS technique may need a separation procedure during real sample analysis.

Conclusion

Resonance Rayleigh scattering is shown to facilitate the determination of several proteins, pesticides, insecticides, metal ions, fungicides and nucleic acid. The determination of these product using RRS technique have reached very low detection limits in a wide concentration range, without any doubts regarding the interference with co-existing substances. Several researchers have proven the feasibility of the RRS technique using nanoparticles as probes in comparison with the analytical method. Although, RRS technique has been successfully applied to determine various analyte in serum sample, the technique cannot be applied to samples that have strong absorption (color) and fluorescence such as blood due to inner filter effects. Hence, RRS technique is very sensitive to several interactions as intermolecular electrostatic attraction,

Table 16 Comparison of the RRS technique in detecting D-2-deoxyribose in deoxyribonucleic acid and D-ribose in ribonucleic acid with other analytical method

	Methods	LOD	Concentration Range
DNA	Electrochemical technique using Au NPs [109]	0.66 ng.mL^{-1}	2.4–244 ng.mL^{-1}
	Electrochemical method using change in flexibility [110]	0.33 ng.mL^{-1}	0.66–132 ng.mL^{-1}
	Colorimetric method [111]	2.8 ng.mL^{-1}	0–33 ng.mL^{-1}
	RRS technique [108]	12 μg.mL^{-1}	10–100 μg.mL^{-1}
RNA	Label free electrochemical method [112]	0.14 fg.mL^{-1}	0.34–34 fg.mL^{-1}
	RRS technique [108]	38 μg.mL^{-1}	10–100 μg.mL^{-1}

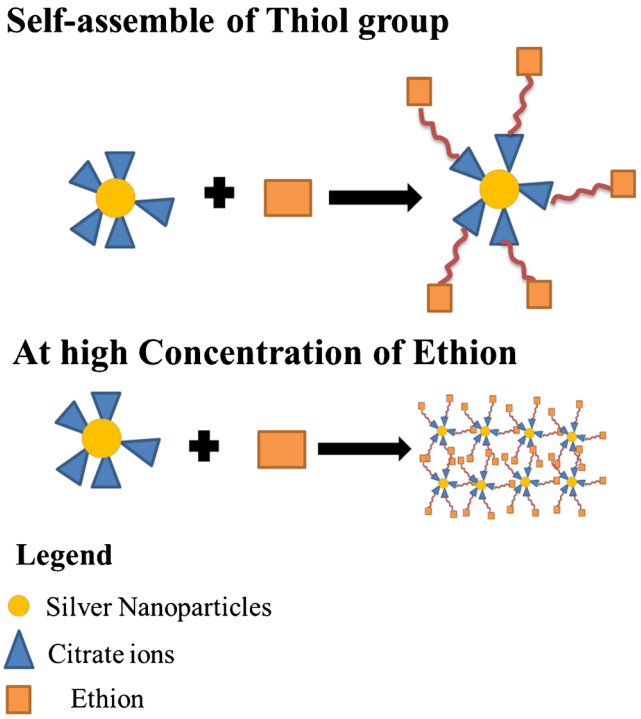

Fig. 9 Self-assemble of thiol group in presence of citrate ions

Table 17 The difference in the concentration range to detect ethion molecules using RRS technique and analytical method

Methods	LOD	Concentration Range
Solid-phase microextraction [115]	22 $\mu g.L^{-1}$	0.1–1 $\mu g.L^{-1}$
GC-FPD [116]	20 $\mu g.L^{-1}$	10–40 $\mu g.L^{-1}$
RRS technique [114]	3.7 $\mu g.L^{-1}$	10–900 $\mu g.L^{-1}$

hydrogen bonding etc. which limits the use of it. Finally, the RRS technique was found to be cheap, fast and easy to manipulate without any pretreatment of the targeted analyte compared to other technique that they are more expensive, time consuming and need several pretreatments.

Compliance with ethical standards The author(s) declare that they have no competing interests.

References

1. Siriwardana K, Nettles CB, Vithanage BCN, Zhou Y, Zou S, Zhang D (2016) On-resonance fluorescence, resonance Rayleigh scattering, and Ratiometric resonance synchronous spectroscopy of molecular- and quantum dot-fluorophores. Anal Chem 88(17): 9199–9206
2. Zimmermann R, Runge E, Savona V (2003) In: Takagahara T (ed) Theory of resonant secondary emission: Rayleigh scattering versus luminescence, in *Quantum Coherence Correlation and Decoherence in Semiconductor Nanostructures*. Elsevier Science, pp 89–165
3. Andrews DL (1999) Rayleigh scattering and Raman effect. Spectroscopy and spectrometry:1993–2000
4. Liu S, Luo H, Li N, Liu Z, Zheng W (2001) Resonance Rayleigh scattering study of the interaction of heparin with some basic diphenyl naphthylmethane dyes. Anal Chem 73(16):3907–3914
5. Stobiecka M, Deeb J, Hepel M (2010) Ligand exchange effects in gold nanoparticle assembly induced by oxidative stress biomarkers: homocysteine and cysteine. Biophys Chem 146:98–107
6. Madrakian T, Bagheri H, Afkhami A, Soleimani M (2014) Spectroscopic and molecular docking techniques study of the interaction between oxymetholone and human serum albumin. J Lumin 155:218–225
7. Ling J, Huang CZ, Li YF, Zhang L, Chen LQ, Zhen SJ (2009) Light-scattering signals from nanoparticles in biochemical assay, pharmaceutical analysis and biological imaging. Trends Anal Chem 28(4):447–453
8. De Carvalho DF, De Medeiros SN, Morales MA, Dantas AL, Carriço AS (2013) Synthesis of magnetite nanoparticles by high energy ball milling. Appl Surf Sci 275:84–87
9. Pérez-Tijerina E, Pinilla MG, Rosales M, Ortiz-Mendez U, Torres A, José-Yacaman M (2008) Highly size-controlled synthesis of au / Pd nanoparticles by inert-gas condensation. Faraday Discuss 138:353–362
10. Lee HS, Zhu L, Weiss RA (2005) Formation of nanoparticles during melt mixing a thermotropic liquid crystalline polyester and sulfonated polystyrene ionomers : morphology and origin of formation. Polymer 46:10841–10853
11. Manawi YM, Ihsanullah SA, Al-Ansari T, Atieh MA (2017) A review of carbon nanomaterials' synthesis via the chemical vapor deposition (CVD) method. Materials 11(822):1–36
12. Reau A, Guizard B, Mengeot C, Boulange L, Ténégal F (2007) Large scale production of nanoparticles by laser pyrolysis. Mater Sci Forum 536:85–88
13. Pingali KC, Deng S, Rockstraw DA (2009) Synthesis of nanowires by spray pyrolysis. Sensors:1–6
14. Soliwoda K, Rosowski M, Tomaszewska T, Tkacz-szczesna B, Celichowski G, Psarski M, Grobelny J (2015) Physicochemical and engineering aspects synthesis of monodisperse gold nanoparticles via electrospray-assisted chemical reduction method in cyclohexane. Colloids Surfaces A: Physicochem Eng Asp 482:148–153
15. Xu H, Zeiger BW, Suslick KS (2013) Sonochemical synthesis of nanomaterials. Chem Soc Rev 42(7):2555–2567
16. Ahlawat DS, Kumari R, Rachna YI (2014) Synthesis and characterization of sol–gel prepared silver nanoparticles. Int J Nanosci 13(1):1–8
17. Aneesh PM, Vanaja KA, Jayaraj MK (2007) Synthesis of ZnO nanoparticles by hydrothermal method. Nanophotonic Mater IV 6639:1–9
18. Ganguli AK, Ahmad T, Vaidya S, Ahmed J (2008) Microemulsion route to the synthesis of nanoparticles. Pure Appl Chem 80(11): 2451–2477
19. Ke Thanh NV (2014) A low cost microwave synthesis method for preparation of gold nanoparticles. Commun Phys 24(2):153–161
20. El Kurdi R, Patra D (2017) The role of OH − in the formation of highly selective gold nanowires at extreme pH: multi-fold enhancement in the rate of the catalytic reduction reaction by gold nanowires. Phys Chem Chem Phys 19(7):5077–5090
21. Gholami-Shabani M, Shams-Ghahfarokhi M, Gholami-Shabani Z, Akbarzadeh A, Riazi G, Ajdari S, Amani A, Razzaghi-Abyaneh M (2015) Enzymatic synthesis of gold nanoparticles using sulfite reductase purified from Escherichia coli: a green eco-friendly approach. Process Biochem 50(7):1076–1085
22. Sehgal N, Soni K, Gupta N, Kanchan K (2018) Microorganism assisted synthesis of gold nanoparticles: a review. Asian J Biomed Pharm Sci 8(64):22–29

23. Mittal AK, Chisti Y, Banerjee UC (2013) Synthesis of metallic nanoparticles using plant extracts. Biotechnol Adv 31(2):346–356
24. Martinez-Abad A (2011) Silver-based antimicrobial polymers for food packaging. Novel materials and nanotechnology:347–367
25. El Kurdi R, Patra D (2018) Tuning the surface of au nanoparticles using poly(ethylene glycol)- block -poly(propylene glycol)- block -poly(ethyleneglycol): enzyme free and label free sugar sensing in serum samples using resonance Rayleigh scattering spectroscopy. Phys Chem Chem Phys 20(14):9616–9629
26. Zhu W, Wang Q, Su D (2013) Study on the interaction between cadmium sulphide nanoparticles and proteins by resonance Rayleigh scattering spectra. J Chem 2013:1–8
27. Zhou J, Ling Y, Li NB, Luo QH (2019) Fluorometric and resonance Rayleigh scattering dual-mode bioprobe for determination of the activity of alkaline phosphatase based on the use of CoOOH nanoflakes and cobalt (II) -dependent DNAzyme-assisted amplification. Michrochem Acta 186(437):1–8
28. Khlebtsov N, Dykman L (2011) Biodistribution and toxicity of engineered gold nanoparticles : a review of in vitro and in vivo studies. Chem Soc Rev 40:1647–1671
29. Sau TK, Rogach AL, Jäckel KTA, Feldmann J (2010) Properties and applications of colloidal nonspherical noble metal nanoparticles. Adv Mater 22(16):1805–1825
30. Reynolds RA, Mirkin CA, Letsinger RL (2000) Homogeneous , nanoparticle-based quantitative colorimetric detection of oligonucleotides. Am Chem Soc 122:3795–3796
31. Lepoitevin M, Lemouel M, Bechelany M, Janot J, Balme S (2015) Gold nanoparticles for the bare-eye based and spectrophotometric detection of proteins , polynucleotides and DNA. Microchim Acta 182:1223–1229
32. Taylor JR, Fang MM, Nie S (2000) Probing specific sequences on single DNA molecules with bioconjugated fluorescent nanoparticles. Anal Chem 72(9):1979–1986
33. Nietzold C, Lisdat F (2012) Fast protein detection using absorption properties of gold nanoparticles†. Analyst 137:2821–2826
34. Obare SO, Hollowell RE, Murphy CJ (2002) Sensing strategy for lithium ion based on gold nanoparticles. Langmuir 18(26):10407–10410
35. Lin SY, Liu SW, Lin CM, Chen CH (2002) Recognition of potassium ion in water by 15-crown-5 functionalized gold nanoparticles. Anal Chem 74(2):330–335
36. Liu S, Yang Z, Liu Z, Kong L (2006) Resonance Rayleigh-scattering method for the determination of proteins with gold nanoparticle probe. Anal Biochem 353(1):108–116
37. Eertmans F, Bogaert V, Puype B (2011) Development and validation of a high-performance liquid chromatography (HPLC) method for the determination of human serum albumin (HSA) in medical devices. Anal Methods 3:1296–1302
38. Chen M, Xiang X, Wu K, He H, Chen H, Ma C (2017) A novel detection method of human serum albumin based on the poly (thymine) - templated copper nanoparticles. Sensors 17:2684–2691
39. Boiero C, Allemandi D, Longhi M, Llabot JM (2015) RP-HPLC method development for the simultaneous determination of timolol maleate and human serum albumin in albumin nanoparticles. J Pharm Biomed Anal 111:186–189
40. Zhang K, Song C, Li Q, Li Y, Jin B (2010) The establishment of a highly sensitive ELISA for detecting bovine serum albumin (BSA) based on a specific pair of monoclonal antibodies (mAb) and its application in vaccine quality control. Hum Vaccin 6(8):652–658
41. Hamidi M, Zarei N (2009) A reversed-phase high-performance liquid chromatography method for bovine serum albumin assay in pharmaceutical dosage forms and protein/antigen delivery systems. Drug Test Anal 1(5):214–218
42. Fischer CR, Müller C, Reber J, Müller A, Krämer SD, Ametamey SM, Schibli R (2012) [18F]fluoro-deoxy-glucose folate: a novel PET radiotracer with improved in vivo properties for folate receptor targeting. Bioconjug Chem 23(4):805–813
43. Qiao J, Dong P, Mu X, Qi L, Xiao R (2016) Biosensors and bioelectronics folic acid-conjugated fl uorescent polymer for up-regulation folate receptor expression study via targeted imaging of tumor cells. Biosens Bioelectron 78:147–153
44. Li H, Cheng Y, Liu Y, Chen B (2016) Fabrication of folic acid-sensitive gold nanoclusters for turn-on fl uorescent imaging of overexpression of folate receptor in tumor cells. Talanta 158:118–124
45. Wu L, Liu Y, Huang R, Zhao H, Shu W (2017) Rapid and selective determination of folate receptor α with sensitive resonance Rayleigh scattering signal. Int J Anal Chem:1–6
46. Li R, Wang C, Hu Y, Zheng O, Guo L, Lin Z, Qiu B, Chen G (2014) Electrochemiluminescence biosensor for folate receptor based on terminal protection of small-molecule-linked DNA. Biosens Bioelectron 58:226–231
47. Zhao J, Hu S, Chen X, Zhang B, Wang K, Liu X (2014) A colorimetric method for the detection of folate receptor based on terminal protectionassisted cascade signal amplification. Sensors Actuators B Chem 202:1243–1247
48. Li H, Qian ZM (2002) Transferrin/transferrin receptor-mediated drug delivery. Med Res Rev 22(3):225–250
49. Gerber CE, Bruchelt G, Götze-Speer B, Speer CP (2000) Detection by ELISA of low transferrin levels in bronchoalveolar secretions of preterm infants. J Immunol Methods 233:41–45
50. Yang L, Wei W, Gao X, Xia J, Tao H (2005) A new antibody immobilization strategy based on electrodeposition of nanometer-sized hydroxyapatite for label-free capacitive immunosensor. Talanta 68(1):40–46
51. Cai HH, Yang PH, Feng J, Cai J (2009) Immunoassay detection using functionalized gold nanoparticle probes coupled with resonance Rayleigh scattering. Sensors Actuators B Chem 135(2):603–609
52. Kurose H (2004) β2adrenergic receptors: structure, regulation and signaling by partial and full agonists. Allergol Int 53(4):321–330
53. Bateman ED, Kornmann O, Schmidt P, Pivovarova A, Engel M, Fabbri LM (2011) Tiotropium is noninferior to salmeterol in maintaining improved lung function in B16-Arg / Arg patients with asthma. J Allergy Clin Immunol 128(2):315–322
54. Bi S, Wang T, Wang T, Zhao T, Zhou H (2015) Spectroscopy using gold nanoparticles as probe for detection of salmeterol xinafoate by resonance Rayleigh light scattering. Spectrochim Acta Part A Mol Biomol Spectrosc 135:1074–1079
55. Murnane D, Martin GP, Marriott C (2006) Validation of a reverse-phase high performance liquid chromatographic method for concurrent assay of a weak base (salmeterol xinafoate) and a pharmacologically active steroid (fluticasone propionate). J Pharm Biomed Anal 40:1149–1154
56. Samir A, Salem H, Abdelkawy M (2012) New developed spectrophotometric method for simultaneous determination of salmeterol xinafoate and fluticasone propionate in bulk powder and Seritide diskus inhalation. Bull Fac Pharmacy Cairo Univ 50(2):121–126
57. Herbst RS (2004) Review of epidermal growth factor receptor biology. Int J Radiat Oncol Biol Phys 59(2):21–26
58. Li J, Yang Y, Wang J, Zhang B, Chang H, Wei W (2018) Resonance Rayleigh scattering detection of the epidermal growth receptor based on an aptamer functionalized gold nanoparticles probe. Anal Methods 10:2910–2916
59. Song J, Shi W, Zhang Y, Sun M, Liang X, Zheng S (2016) Epidermal growth factor receptor and B7-H3 expression in esophageal squamous tissues correlate to patient prognosis. Onco Targets Ther 9:6257–6263

60. Ilkhani H, Sarparast M, Noori A, Bathaie SZ, Mousavi MF (2015) Electrochemical aptamer/antibody based sandwich immunosensor for the detection of EGFR, a cancer biomarker, using gold nanoparticles as a signaling probe. Biosens Bioelectron 74:491–497
61. Regiart M, Fernández-Baldo MA, Villarroel-Rocha J, Messina GA, Bertolino FA, Sapag K, Timperman AT, Raba J (2017) Microfluidic immunosensor based on mesoporous silica platform and CMK-3/poly-acrylamide-co-methacrylate of dihydrolipoic acid modified gold electrode for cancer biomarker detection. Anal Chim Acta 96:83–92
62. Berlina AN, Zherdev AV, Dzantiev BB (2019) Progress in rapid optical assays for heavy metal ions based on the use of nanoparticles and receptor molecules. Microchim Acta 186(3):1–39
63. Li ZP, Duan XR, Liu CH, Du BA (2006) Selective determination of cysteine by resonance light scattering technique based on self-assembly of gold nanoparticles. Anal Biochem 351:18–25
64. Lin BL, Colón LA, Zare RN (1994) Dual electrochemical detection of cysteine and cystine in capillary zone electrophoresis. J Chromatogr A 680(1):263–270
65. Chen S, Gao H, Shen W, Lu C, Yuan Q (2019) Colorimetric detection of cysteine using noncrosslinking aggregation of fluorosurfactant-capped silver nanoparticles. Sensors Actuators B Chem 190:673–678
66. Parham H, Pourreza N, Marahel F (2015) Determination of thiram using gold nanoparticles and resonance Rayleigh scattering method. Talanta 141:143–149
67. Aulakh JS, Malik AK, Mahajan RK (2005) Solid phase microextraction-high pressure liquid chromatographic determination of Nabam, Thiram and Azamethiphos in water samples with UV detection: preliminary data. Talanta 66(1):266–270
68. Giannoulis KM, Giokas DL, Tsogas GZ, Vlessidis AG (2014) Ligand-free gold nanoparticles as colorimetric probes for the non-destructive determination of total dithiocarbamate pesticides after solid phase extraction. Talanta 119:276–283
69. Amorello D, Orecchio S (2013) Micro-determination of dithiocarbamates in pesticide formulations using voltammetry. Microchem J 110:334–339
70. Flitsch SL, Ulijn RV (2003) Sugars tied to the spot. Nature 421: 219–220
71. Huang Z, Zheng L, Feng F, Chen Y, Wang Z, Lin Z, Lin X, Weng S (2018) A simple and effective colorimetric assay for glucose based on MnO2 nanosheets. Sensors 18(8):1–11
72. Manso J, Mena ML, Yáñez-Sedeño P, Pingarrón J (2007) Electrochemical biosensors based on colloidal gold-carbon nanotubes composite electrodes. J Electroanal Chem 603(1):1–7
73. Duarte-Delgado D, Narváez-Cuenca CE, Restrepo-Sánchez LP, Kushalappa A, Mosquera-Vásquez T (2015) Development and validation of a liquid chromatographic method to quantify sucrose, glucose, and fructose in tubers of Solanum tuberosum group Phureja. J Chromatogr B 975:18–23
74. El Kurdi R, Patra D (2017) Amplification of resonance Rayleigh scattering of gold nanoparticles by tweaking into nanowires: biosensing of atocopherol by enhanced resonance Rayleigh scattering of curcumin capped gold nanowires through non-covalent interaction. Talanta 168:82–90
75. Brabcová I, Kovářová L, Šatínský D, Havlíková L, Solich P (2013) A fast HPLC method for determination of vitamin E acetate in dietary supplements using monolithic column. Food Anal Methods 6(2):380–385
76. Korchazhkina O, Jones E, Czauderna M, Spencer SA, Kowalczyk J (2006) HPLC with UV detection for measurement of vitamin E in human milk. Acta Chromatogr 16(16):48–57
77. Yamamoto K, Kotani A, Hakamata H (2018) Electrochemical detection of tocopherols in vegetable oils by supercritical fluid chromatography equipped with carbon fiber electrodes. Anal Methods 10(36):4414–4418
78. Arora S, Lidor A, Abularrage CJ, Weiswasser JM, Nylen E, Kellicut D, Sidawy AN (2006) Thiamine (vitamin B1) improves endothelium-dependent vasodilatation in the presence of hyperglycemia. Ann Vasc Surg 20(5):653–658
79. Liu S, Chen S, Liu Z, Hu X, Wang F (2006) A highly sensitive resonance Rayleigh scattering method for the determination of vitamin B1 with gold nanoparticles probe. Microchim Acta 154(1):87–93
80. Zou J, Lan Chen X (2007) Using silica nanoparticles as a catalyst carrier to the highly sensitive determination of thiamine. Microchem J 86(1):42–47
81. Li Y, Wang P, Wang X, Cao M, Xia YS, Cao C, Liu MG, Zhu CQ (2010) An immediate luminescence enhancement method for determination of vitamin B1 using long-wavelength emitting water-soluble CdTe nanorods. Microchim Acta 169(1):65–71
82. Molina-Delgado MA, Aguilar-Caballos MP, Gómez-Hens A (2016) Simultaneous photometric microplate assay for free and total thiamine using gold nanoparticles and alkaline phosphatase. Microchim Acta 183(4):1385–1390
83. Tchounwou PB, Yedjou CG, Patlolla AK, Sutton DJ (2013) Heavy metals toxicity and the environment. Natl Inst Heal 47(10):1–30
84. Ouyang H, Li C, Liu Q, Wen G, Liang A, Jiang Z (2017) Resonance Rayleigh scattering and SERS spectral detection of trace hg(II) based on the gold Nanocatalysis. Nanomaterials 7(114):1–10
85. Gao ZF, Song WW, Luo HQ, Li NB (2015) Detection of mercury ions (II) based on non-cross-linking aggregation of double-stranded DNA modified gold nanoparticles by resonance Rayleigh scattering method. Biosens Bioelectron 65:360–365
86. Matlou GG, Nkosi D, Pillay K, Arotiba O (2016) Electrochemical detection of hg(II) in water using self-assembled single walled carbon nanotubepoly(m-amino benzene sulfonic acid) on gold electrode. Sens Bio-Sensing ReS 10:27–33
87. Ichinoki S, Kitahata N, Fujii Y (2004) Selective determination of mercury(II) ion in water by solvent extraction followed by reversed-phase HPLC. J Liq Chromatogr Relat Technol 27(11): 1785–1798
88. Vallant B, Kadnar R, Goessler W (2007) Development of a new HPLC method for the determination of inorganic and methylmercury in biological samples with ICP-MS detection. J Anal At Spectrom 22(3):322–325
89. Wygladacz K, Radu A, Xu C, Qin Y, Bakker E (2005) Fiber-optic microsensor array based on fluorescent bulk optode microspheres for the trace analysis of silver ions. Anal Chem 77(15):4706–4712
90. Wen G, Lin C, Tang M, Liu G, Liang A, Jiang Z (2013) A highly sensitive aptamer method for ag+sensing using resonance Rayleigh scattering as the detection technique and a modified nanogold probe. R Soc Chem Adv 3(6):1941–1946
91. Lin YH, Tseng WL (2009) Highly sensitive and selective detection of silver ions and silver nanoparticles in aqueous solution using an oligonucleotidebased fluorogenic probe. Chem Commun 43:6619–6621
92. Wu C, Xiong C, Wang L, Lan C, Ling L (2010) Sensitive and selective localized surface plasmon resonance light-scattering sensor for ag+with unmodified gold nanoparticles. Analyst 135(10): 2682–2687
93. Aragay G, Pons J, Merkoçi A (2011) Recent trends in macro-, micro-, and nanomaterial-based tools and strategies for heavy-metal detection. Chem Rev 111(5):3433–3458
94. Sughis M, Nawrot TS, Haufroid V, Benoit N (2012) Adverse health effects of child labor: high exposure to chromium and oxidative DNA damage in children manufacturing surgical instruments. Environ Health Perspect 120(10):1469–1474
95. Chen M, Cai HH, Yang F, Lin D, Yang PH, Cai J (2014) Highly sensitive detection of chromium (III) ions by resonance Rayleigh

scattering enhanced by gold nanoparticles. Spectrochim Acta - Part A Mol Biomol Spectrosc 118:776–781
96. Elmizadeh H, Soleimani M, Faridbod F, Bardajee GR (2018) A sensitive nano-sensor based on synthetic ligand-coated CdTe quantum dots for rapid detection of Cr(III) ions in water and wastewater samples. Colloid Polym Sci 296(9):1581–1590
97. Prabhakaran DC, Riotte J, Sivry Y, Subramanian S (2017) Electroanalytical detection of Cr(VI) and Cr(III) ions using a novel microbial sensor. Electroanalysis 29(5):1222–1231
98. Liang A, Wei Y, Wen G, Yin W, Jiang Z (2013) A new resonance Rayleigh scattering method for trace Pb, coupling the hydride generation reaction with nanogold formation. RSC Adv3(31): 12585–12588
99. Li C, Fan P, Liang A, Liu Q, Jiang Z (2018) Aptamer based determination of Pb(II) by SERS and by exploiting the reduction of HAuCl4 by H2O2 as catalyzed by graphene oxide nanoribbons. Microchim Acta 185(3):1–11
100. Salih FE, Ouarzane A, El RM (2017) Electrochemical detection of lead (II) at bismuth/poly(1,8-diaminonaphthalene) modified carbon paste electrode. Arab J Chem 10(5):596–603
101. Kuang H, Xing C, Hao C, Liu L, Wang L, Xu C (2013) Rapid and highly sensitive detection of lead ions in drinking water based on a strip immunosensor. Sensors 13(4):4214–4224
102. Youqiu H, Shaopu L, Qin L, Zhongfang L, Xiaoli H (2005) Absorption, fluorescence and resonance Rayleigh scattering spectral characteristics of interaction of gold nanoparticle with safranine T. Sci China Ser B 48(3):216–226
103. Abd Alkhlig A, Bakheet A (2017) Determination of rhodamine B pigment in food samples by ionic liquid coated magnetic Core/Shell Fe3O4@SiO2Nanoparticles coupled with fluorescence spectrophotometry. Am J Heterocycl Chem 5(1):60–66
104. Wang W, Zhu X, Yan C (2013) Determination of safranine T in food samples by CTAB sensitised fluorescence quenching method of the derivatives of calix[4]arene. Food Chem 141(3):2207–2212
105. Han X, Wang H, Ou X, Zhang X (2012) Highly sensitive, reproducible, and stable SERS sensors based on well-controlled silver nanoparticledecorated silicon nanowire building blocks. J Mater Chem 22(28):14127–14132
106. Smitha SL, Nissamudeen KM, Philip D, Gopchandran KG (2008) Studies on surface plasmon resonance and photoluminescence of silver nanoparticles. Spectrochim Acta - Part A Mol Biomol Spectrosc 71(1):186–190
107. Carrey EA, Simmonds HA (2005) Nucleic Acid Med Bioch:121–140
108. El Khoury E, Abiad M, Kassaify ZG, Patra D (2015) Green synthesis of curcumin conjugated nanosilver for the applications in nucleic acid sensing and anti-bacterial activity. Colloids Surfaces B Biointerfaces 127:274–280
109. Peng H, Soeller C, Cannell MB, Bowmaker GA, Cooney RP, Travas-Sejdic J (2006) Electrochemical detection of DNA hybridization amplified by nanoparticles. Biosens Bioelectron 21(9): 1727–1736
110. Liu X, Qu X, Dong J, Ai S, Han R (2011) Electrochemical detection of DNA hybridization using a change in flexibility. Biosens Bioelectron 26(8):3679–3682
111. Li H, Rothberg L (2004) Colorimetric detection of DNA sequences based on electrostatic interactions with unmodified gold nanoparticles. Proc Natl Acad Sci 101(39):14036–14039
112. Song T, Guo X, Li X, Zhang S (2016) Label-free electrochemical detection of RNA based on 'Y' junction structure and restriction endonucleaseaided target recycling strategy. J Electroanal Chem 781:251–256
113. Salas JH, González MM, Noa M, Pérez NA, Díaz G, Gutiérrez R, Zazueta H, Osun I (2003) Organophosphorus pesticide residues in Mexican commercial pasteurized milk. J Agric Food Chem 51(15):4468–4471
114. Parham H, Saeed S (2015) Resonance Rayleigh scattering method for determination of ethion using silver nanoparticles as probe. Talanta 131:570–576
115. Lambropoulou DA, Albanis TA (2004) Optimization of headspace solid-phase microextraction conditions for the determination of organophosphorus insecticides in olive oiL. Int J Environ Anal Chem 84:243–255
116. Liu H, Kong W, Qi Y, Gong B, Miao Q, Wei J, Yang M (2014) Streamlined pretreatment and GC-FPD analysis of multi-pesticide residues in perennial Morinda roots: a tropical or subtropical plant. Chemosphere 95:33–40